Set-Invariance Based Fuzzy Output Tracking Control for Vehicle Autonomous Driving under Uncertain Lateral Forces and Steering Constraints

Anh-Tu Nguyen*, Thierry-Marie Guerra*, Jagat Rath†, Hui Zhang‡, Reinaldo Palhares§
*Laboratory LAMIH UMR CNRS 8201, Université Polytechnique Hauts-de-France, France
†Department of Informatics, Technische Universitat München, Germany
‡School of Transportation Science and Engineering, Beihang University, China
§Department of Electronics Engineering, Federal University of Minas Gerais, Brazil
E-mail: nguyen.trananhtu@gmail.com

***Abstract*—This paper presents a new control method for path tracking of autonomous vehicles. Takagi-Sugeno fuzzy control is used to handle the time-varying vehicle speed and the uncertain tire-road forces involved in the nonlinear vehicle dynamics. To avoid using costly vehicle sensors while keeping a simple control structure, a new fuzzy static output feedback (SOF) scheme is proposed. Moreover, robust set-invariance is exploited to take into account the physical limitations on the steering input and the vehicle state in the control design for safety and comfort improvement. Based on Lyapunov stability arguments, a non-parallel distributed compensation SOF controller is designed for autonomous driving with reduced conservatism. The control design is reformulated as an optimization problem under linear matrix inequalities, easily solved with available numerical solvers. The path tracking performance of the proposed fuzzy controller is evaluated via dynamic driving tests conducted with high-fidelity CarSim/Simulink co-simulations.**

***Index Terms*—Fuzzy systems, fuzzy control, autonomous vehicles, path tracking, vehicle dynamics, vehicle control.**

I. Introduction

Autonomous ground vehicles have been considered as a promising solution to improve not only the safety, accessibility and comfort of passengers but also the energy-saving efficiency [1]. For these reasons, autonomous driving technology has received a great deal of attention from academic researchers, industrial companies and local governments. As one of the most important parts of vehicle autonomous navigation, path tracking of autonomous vehicles has been a significant research topic [2]–[4]. The key control goal is to achieve path following performance with acceptably small tracking errors and smooth steering actions under various driving conditions [4]. Remarkable contributions on path tracking of autonomous vehicles have been reported in the literature. Generally speaking, the path tracking control strategies can be classified into three main categories: model-free control, kinematic-based control and feedback control. First, model-free controllers, such as PID control [5] or fuzzy logic control [6], [7], generate the steering actions based on the tracking errors. Without taking into account the information of vehicle dynamics in the design, these control methods require a costly tuning task to achieve an acceptable path tracking performance [8]. Second, the kinematic-based controllers are designed using a vehicle kinematics model and/or geometric relations [9]. Despite their simplicity, these control approaches only demonstrate their capabilities for low-speed driving situations. Third, the feedback control designs are based on the vehicle dynamics which can be used to overcome the above-mentioned drawbacks [4].

Numerous works on path tracking feedback control of autonomous vehicles have been proposed, which are mostly based on conventional control theory [8], [9]. Sliding mode control technique was applied to vehicle control in [10]. Despite its robustness with respect to uncertainties and disturbances, the involved chattering issue still leads to both theoretical and practical difficulties [8]. An active disturbance rejection control (ADRC) was developed in [11] for vehicle steering control in the presence of uncertainties and external disturbance. Note that ADRC controllers require a heavy tuning task to achieve a satisfactory control performance. Model predictive control (MPC) has been largely applied to path tracking and obstacle avoidance of autonomous vehicles [12]–[14]. However, MPC technique requires solving an on-line optimization problem at each control step, which leads expensive computational cost for real-time implementation, especially for nonlinear MPC schemes. Takagi-Sugeno (TS) fuzzy approaches [15] have been proposed to deal with the vehicle tracking control issues [3], [16], [17]. In contrast to model-free fuzzy control [6], [18], stability and robustness analysis can be achieved with TS fuzzy control approaches [19], [20]. However, fuzzy model-based output feedback control for uncertain systems remains challenging [21].

Despite a great advance, the following issues related to path tracking control for autonomous driving still remain challenging. First, requiring full-state information for feedback design is a strong assumption within vehicle control context due to the sensor cost reasons [9]. The second challenge is the reliance of the control design on the vehicle modeling. Using an accurate vehicle model may lead to major difficulties for the control design task due to the strong coupling nonlinearities. Hence, the design of a model-based controller robust to the unmodeled vehicle dynamics, time-varying parameters and external disturbances, is of crucial importance [22]. The third

978-1-7281-6932-3/20/$31.00 ©2020 IEEE

challenge consists in considering the physical limitations, *e.g.*, steering saturation, in the control design to improve the driving safety and comfort. This important issue has not been well addressed for robust output feedback control schemes [23]–[26]. In particular, most of existing constrained path following control for autonomous vehicles are mainly based state-feedback control schemes [3].

This paper presents a new fuzzy SOF controller to *simultaneously* address the three above challenges of autonomous path following control. Robust TS fuzzy model-based technique is used to deal with the nonlinear uncertain vehicle dynamics. Then, the time-varying feature of the vehicle speed and the highly uncertain behaviors of the lateral tire-road forces can be taken into account in the control design to improve the path tracking performance. Moreover, exploiting the robust set-invariance property and Lyapunov stability arguments, the steering input saturation can be explicitly considered in the control design for safety and confort reasons. Differently from [27], [28], here a fuzzy Lyapunov function and a non-parallel distributed compensation (non-PDC) scheme are used to reduce further the design conservatism. The control design procedure is recast as an optimization problem under linear matrix inequalities (LMIs) with a single parameter line search, which can be easily solved with available solvers [29]. The effectiveness of the proposed TS fuzzy SOF controller is clearly demonstrated using high-fidelity CarSim/Simulink co-simulations under dynamic driving conditions. It is important to note that this conference paper is a short version of the work [30]. More technical extensions and details on control validations can be found in [30].

Notation. For a vector x, x_i denotes its ith entry. For a square matrix X, $X^\top$ denotes its transpose, $X \succ 0$ means that X is positive definite, $X_{(i)}$ denotes its ith row and $\mathrm{He}\, X = X + X^\top$. $\mathrm{diag}(X_1, X_2)$ denotes a block-diagonal matrix composed of X_1, X_2. I denotes the identity matrix of appropriate dimension. The set of nonnegative integers is denoted by $\mathbb{Z}_+$. For $N \in \mathbb{Z}_+$, we denote $\mathcal{I}_N = \{1, \ldots, r\} \subset \mathbb{Z}_+$. The symbol '$\star$' stands for the terms deduced by symmetry in symmetric block matrices. For brevity, the following notation for convex sums is adopted:

$$\begin{aligned}
\Pi_h &= \sum_{i=1}^{r} h_i(\theta)\Pi_i, \qquad \Pi_h^{-1} = \left(\sum_{i=1}^{r} h_i(\theta)\Pi_i\right)^{-1},\\
\Sigma_{hh} &= \sum_{i=1}^{r}\sum_{j=1}^{r} h_i(\theta)h_j(\theta)\Sigma_{ij},\\
\Phi_{hhh} &= \sum_{i=1}^{r}\sum_{j=1}^{r}\sum_{k=1}^{r} h_i(\theta)h_j(\theta)h_k(\theta)\Phi_{ijk}.
\end{aligned} \tag{1}$$

with Π_i, Σ_{ij} and Φ_{ijk} are matrices of appropriate dimensions.

II. Vehicle Modeling and Problem Formulation

We present hereafter the vehicle modeling for path tracking control, see Fig. 1. The nomenclature is given in Table I.

TABLE I
Vehicle Nomenclature.

Symbol	Description
v_x/v_y	longitudinal/lateral speed
β	sideslip angle at the center of gravity (CG)
r	vehicle yaw rate
y_L	lateral deviation error
ψ_L	heading error
δ	steering angle
M	total mass of the vehicle
l_f/l_r	distance from CG to the front/rear axle
l_s	look-ahead distance
I_z	vehicle yaw moment of inertia
$\mathscr{C}_f/\mathscr{C}_r$	front/rear cornering stiffness

A. Road-Vehicle Model

A non-linear single track vehicle model is used to study the vehicle motions, whose dynamics is given as follows [3]:

$$\begin{aligned}
M(\dot{v}_x - r v_y) &= F_{xf}\cos\delta - F_{yf}\sin\delta + F_{xr},\\
M(\dot{v}_y + r v_x) &= F_{xf}\sin\delta + F_{yf}\cos\delta + F_{yr},\\
I_z\dot{r} &= l_f(F_{xf}\sin\delta + F_{yf}\cos\delta) - l_r F_{yr}.
\end{aligned} \tag{2}$$

The front and rear longitudinal forces F_{xi} and lateral forces F_{yi}, for $i \in \{f, r\}$, are caused by the tire-road interaction. The behaviors of these forces are highly nonlinear and depend on several factors, for instance slip angles, tire/road characteristics, normal load [31]. To reduce the design complexity, the following norm-bounded uncertain tire model is used [22]:

$$\begin{aligned}
F_{yf} &= 2\mathscr{C}_f\alpha_f = 2\mathscr{C}_f\left(\delta - \frac{v_y + l_f r}{v_x}\right),\\
F_{yr} &= 2\mathscr{C}_r\alpha_r = 2\mathscr{C}_r\frac{l_r r - v_y}{v_x}.
\end{aligned} \tag{3}$$

where the cornering stiffness are time-varying to take into account the road friction changes or the nonlinear tire behaviors [32]. These bounded parameters $\mathscr{C}_f \in [\mathscr{C}_{f\min}, \mathscr{C}_{f\max}]$ and $\mathscr{C}_r \in [\mathscr{C}_{r\min}, \mathscr{C}_{r\max}]$, can be represented by

$$\mathscr{C}_f = C_f + \Delta C_f\zeta_f(t), \quad \mathscr{C}_r = C_r + \Delta C_r\zeta_r(t), \tag{4}$$

where $|\zeta_i(t)| \le 1$, $i \in \{f, r\}$, are *unknown* parameters, and

$$\begin{aligned}
C_f &= \frac{\mathscr{C}_{f\max} + \mathscr{C}_{f\min}}{2}, \qquad C_r = \frac{\mathscr{C}_{r\max} + \mathscr{C}_{r\min}}{2},\\
\Delta C_f &= \frac{\mathscr{C}_{f\max} - \mathscr{C}_{f\min}}{2}, \quad \Delta C_r = \frac{\mathscr{C}_{r\max} - \mathscr{C}_{r\min}}{2}.
\end{aligned}$$

For steering control purposes, we consider the small angles assumption and a slow vehicle speed variation. Then, the vehicle lateral dynamics can be derived from (2) and (3) as follows [33], [34]:

$$\begin{bmatrix}\dot{\beta}\\ \dot{r}\end{bmatrix} = \begin{bmatrix}-\frac{2(\mathscr{C}_r+\mathscr{C}_f)}{Mv_x} & \frac{2(l_r\mathscr{C}_r - l_f\mathscr{C}_f)}{Mv_x^2} - 1\\ \frac{2(l_r\mathscr{C}_r - l_f\mathscr{C}_f)}{I_z} & \frac{-2(l_r^2\mathscr{C}_r + l_f^2\mathscr{C}_f)}{I_z v_x}\end{bmatrix}\begin{bmatrix}\beta\\ r\end{bmatrix} + \begin{bmatrix}\frac{2\mathscr{C}_f}{Mv_x}\\ \frac{2l_f\mathscr{C}_f}{I_z}\end{bmatrix}\delta \tag{5}$$

where $v_y = v_x\beta$. The vehicle positioning on the road can be represented by the following dynamics [3]:

$$\dot{y}_L = v_x\beta + l_s r + v_x\psi_L, \quad \dot{\psi}_L = r - v_x\rho_r, \tag{6}$$

where the road curvature ρ_r can be obtained from cameras.

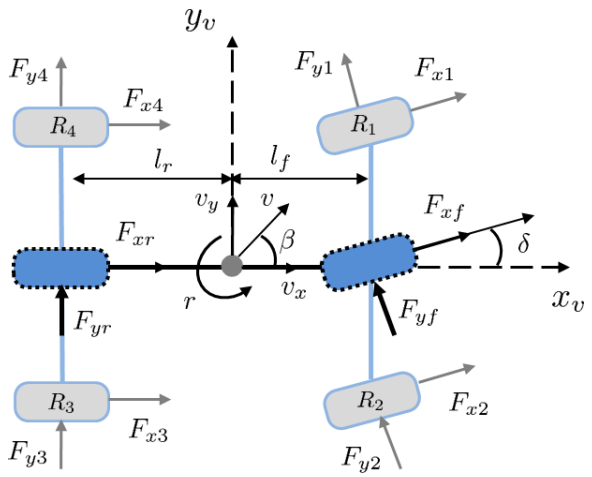

Fig. 1. Schematic of vehicle lateral dynamics.

B. Vehicle Control-Based Model

From the vehicle model (5), the dynamics for path tracking (6), the road-vehicle model can be represented as follows:

$$\dot{x}(t) = \hat{A}_v(t)x(t) + \hat{B}_v(t)\delta(t) + E_v(t)w(t), \tag{7}$$

where $x = \begin{bmatrix}\beta & r & \psi_L & y_L\end{bmatrix}^\top$ is the vehicle state, $w = \rho_r$ is the system disturbance. The steering control input $\delta(t)$ of the vehicle system (7) is subject to actuator saturation

$$\delta(t) = \text{sat}(u(t)) = \text{sign}(u(t)) \min\left(|u(t)|, \delta_{\max}\right),$$

where u is the steering control angle with its maximal physical limitation $\delta_{\max}$. The matrices of system (7) are given by $\hat{A}_v(t) = A_v(t) + \Delta A_v(t)$, $\hat{B}_v(t) = B_v(t) + \Delta B_v(t)$ with

$$A_v = \begin{bmatrix} a_{11} & a_{12} & 0 & 0 \\ a_{21} & a_{22} & 0 & 0 \\ 0 & 1 & 0 & 0 \\ v_x & l_s & v_x & 0 \end{bmatrix}, \; B_v = \begin{bmatrix} b_1 \\ b_2 \\ 0 \\ 0 \end{bmatrix}, \; E_v = \begin{bmatrix} 0 \\ 0 \\ -v_x \\ 0 \end{bmatrix},$$

and

$$a_{11} = -\frac{2(C_r + C_f)}{Mv_x}, \quad a_{12} = \frac{2(l_rC_r - l_fC_f)}{Mv_x^2} - 1,$$
$$a_{21} = \frac{2(l_rC_r - l_fC_f)}{I_z}, \quad a_{22} = \frac{-2(l_r^2C_r + l_f^2C_f)}{I_zv_x},$$
$$b_1 = \frac{2C_f}{Mv_x}, \qquad b_2 = \frac{2l_fC_f}{I_z}.$$

Moreover, ΔA_v and ΔB_v represent the system norm-bounded uncertainties caused by $\mathscr{C}_f$ and $\mathscr{C}_r$ in (4), represented as

$$\Delta A_v(t) = H_v\Delta(t)L_v, \quad \Delta B_v(t) = H_v\Delta(t)N_v,$$

with

$$H_v = \begin{bmatrix} \frac{2\Delta C_r}{Mv_x} & \frac{2\Delta C_f}{Mv_x} \\ -\frac{2\Delta C_r l_r}{I_z} & \frac{2\Delta C_f l_f}{I_z} \\ 0 & 0 \\ 0 & 0 \end{bmatrix}, \quad L_v = \begin{bmatrix} -1 & -1 \\ \frac{l_r}{v_x} & -\frac{l_f}{v_x} \\ 0 & 0 \\ 0 & 0 \end{bmatrix}^\top,$$
$$\Delta(t) = \text{diag}(\zeta_r(t), \zeta_f(t)), \qquad N_v = \begin{bmatrix}0 & 1\end{bmatrix}^\top.$$

For real-time implementation, the control design is performed in the discrete-time domain. Then, the Euler's discretization is used to transform system (7) into its discrete-time counterpart

$$x(\kappa+1) = \hat{A}(v_x)x(\kappa) + \hat{B}(v_x)\text{sat}(u(\kappa)) + E(v_x)w(\kappa). \tag{8}$$

where $\hat{A}(v_x) = I + T_e\hat{A}_v(v_x)$, $\hat{B}(v_x) = T_e\hat{B}_v(v_x)$ and $E(v_x) = T_eE_v(v_x)$. The value of the sampling time is selected as $T_e = 0.01$ [s], which is compatible with real-time hardware setup [3]. Due to the cost reason, the measurement of β is *unavailable* in practice [27]. Then, the vehicle output is defined as

$$y = \begin{bmatrix} 0 & 1 & 0 & 0 \\ 0 & 0 & 1 & 0 \\ 0 & 0 & 0 & 1 \end{bmatrix} x = Cx.$$

The controlled output vector z is defined such that it can represent both the path following performance (via ψ_L and y_L) and the driving comfort (via the lateral acceleration $a_y \simeq v_x r$)

$$z = \begin{bmatrix} \psi_L \\ y_L \\ a_y \end{bmatrix} = \begin{bmatrix} 0 & 0 & 1 & 0 \\ 0 & 0 & 0 & 1 \\ 0 & v_x & 0 & 0 \end{bmatrix} x = D(v_x)x. \tag{9}$$

III. Set-Invariance Based Output Feedback Control for Constrained Fuzzy Systems

This section formulates the fuzzy SOF control problem for autonomous driving under uncertainties and constraints.

A. System Description

We consider the following class of uncertain input-constrained TS fuzzy systems with N inference rules [15]:

$$\begin{aligned} \text{Rule } \mathcal{R}_i: \text{ If } \theta_1(\kappa) \text{ is } \mathcal{M}_1^i \text{ and} \ldots \text{and } \theta_p(\kappa) \text{ is } \mathcal{M}_p^i. \text{ Then} \\ x(\kappa+1) = \hat{A}_i(\kappa)x(\kappa) + \hat{B}_i(\kappa)\text{sat}(u(\kappa)) + E_iw(\kappa) \\ z(\kappa) = D_ix(\kappa), \quad y(\kappa) = Cx(\kappa), \end{aligned} \tag{10}$$

where $x(\kappa) \in \mathbb{R}^{n_x}$ is the state vector, $u(\kappa) \in \mathbb{R}^{n_u}$ the control input, $w(\kappa) \in \mathbb{R}^{n_w}$ the system disturbance, $z(\kappa) \in \mathbb{R}^{n_z}$ the controlled output, and $y(\kappa) \in \mathbb{R}^{n_y}$ the measured output, and $\hat{A}_i(\kappa) = A_i + \Delta A_i(\kappa)$, $\hat{B}_i(\kappa) = B_i + \Delta B_i(\kappa)$. The vector of premise variables is defined as $\theta(\kappa) = [\theta_1(\kappa) \cdots \theta_p(\kappa)]^\top \in \mathbb{R}^p$. The ith local matrices with appropriate dimensions $(A_i, B_i, C_i, D_i, E_i)$ are known constant. Using notation (1), the fuzzy system (10) can be rewritten in the compact form

$$\begin{aligned} x(\kappa+1) = \hat{A}_hx(\kappa) + \hat{B}_h\text{sat}(u(\kappa)) + E_hw(\kappa) \\ z(\kappa) = D_hx(\kappa), \quad y(\kappa) = Cx(\kappa), \end{aligned} \tag{11}$$

where the uncertain state-space matrices satisfy

$$\begin{aligned} \hat{A}_h = A_h + \Delta A(\kappa), \qquad \hat{B}_h = B_h + \Delta B(\kappa), \\ \Delta A(\kappa) = H_h\Delta(\kappa)L_h, \qquad \Delta B(\kappa) = H_h\Delta(\kappa)N_h. \end{aligned} \tag{12}$$

The constant matrices with proper dimensions H_i, L_i, N_i, $i \in \mathcal{I}_N$, in (12), are known, and the time-varying uncertain matrix satisfies $\Delta(\kappa)^\top\Delta(\kappa) \preceq I$. The membership functions (MFs) $h_i(\theta)$, for $i \in \mathcal{I}_N$, satisfy the convex sum property

$$\sum_{i=1}^{N} h_i(\theta) = 1, \quad 0 \le h_i(\theta) \le 1, \quad \forall i \in \mathcal{I}_N.$$

The input saturation function is defined as

$$\mathrm{sat}(u_l(\kappa)) = \mathrm{sign}(u_l(\kappa))\min(|u_l(\kappa)|, \bar{u}_l), \quad \kappa \in \mathbb{Z}_+,$$

where the control bounds $\bar{u}_l > 0$, for $\forall l \in \mathcal{I}_{n_u}$, are given. The system disturbance w in (11) is bounded in amplitude as

$$\mathcal{W}_\phi^\infty = \left\{ w : \ \mathbb{R}^+ \to \mathbb{R}^{n_w}, \quad w(\kappa)^\top w(\kappa) \le \phi, \ \kappa \in \mathbb{Z}_+ \right\},$$

with a positive scalar $\phi > 0$.

We consider the following non-PDC control law incorporating the road curvature information as a feedforward action to improve the path following performance [9]:

$$u(\kappa) = F_h G_h^{-1} y(\kappa) + K_h w(\kappa), \tag{13}$$

where the MF-dependent matrices F_h, G_h and K_h of appropriate dimensions are to be determined. Let us define $\psi(u(\kappa)) = u(\kappa) - \mathrm{sat}(u(\kappa))$. From (11) and (13), the closed-loop fuzzy system can be expressed as follows:

$$\begin{aligned} x(\kappa+1) &= A_{cl}(h)x(\kappa) + E_{cl}(h)w(\kappa) - \hat{B}_h\psi(u(\kappa)) \\ z(\kappa) &= D_h x(\kappa), \quad y(\kappa) = Cx(\kappa), \end{aligned} \tag{14}$$

with $A_{cl}(h) = \hat{A}_h + \hat{B}_h F_h G_h^{-1} C$, $E_{cl}(h) = E_h + \hat{B}_h K_h$. For the control design, we consider the following MF-dependent Lyapunov candidate function:

$$V(x) = x^\top Q_h^{-1} x, \quad Q_i \succ 0, \quad \forall i \in \mathcal{I}_N.$$

We define the level set associated with $V(x)$ as

$$\mathscr{L}_V = \{ x \in \mathbb{R}^{n_x} : \ V(x) \le 1, \ \text{for } \forall h \in \Omega \}. \tag{15}$$

The set $\mathscr{L}_V$ is said to be *robustly invariant* w.r.t. the closed-loop system (14) if there exist positive scalars α, τ such that

$$\Delta V + \alpha(V(x(\kappa)) - 1) + \tau(\phi - w(\kappa)^\top w(\kappa)) < 0, \tag{16}$$

where $\Delta V = V(x(\kappa+1)) - V(x(\kappa))$, for $\forall \kappa \in \mathbb{Z}_+$, $\forall x(\kappa) \in \mathscr{L}_V \backslash \{0\}$, $\forall w(\kappa) \in \mathcal{W}_\phi^\infty$. Note that condition (16) guarantees that any closed-loop trajectory of (14) initialized in $\mathscr{L}_V$ will remain within this set for $\forall w(\kappa) \in \mathcal{W}_\phi^\infty$ and $\forall \kappa \in \mathbb{Z}_+$. More details on the set invariance property can be found in [35].

We consider the following control problem.

Problem 1. Determine the MF-dependent matrices F_h, G_h and K_h of the non-PDC SOF controller (13) such that the set $\mathscr{L}_V$ defined in (15) is robustly invariant w.r.t. the TS fuzzy system (14). Moreover, the $\mathcal{L}_\infty-$norm of the controlled output z is bounded as $z^\top z \le \gamma$, for $\gamma > 0$.

Remark that minimizing the $\mathcal{L}_\infty-$norm upper bound γ leads to a better control performance. The following technical lemma [36], extended from the result on modified sector condition in [37], is useful for theoretical developments.

Lemma 1. Consider a matrix M_h and the following set:

$$\mathscr{S}_u = \left\{ x \in \mathbb{R}^{n_x} : \left| M_h Q_h^{-1} x \right| \preceq \bar{u} \right\}.$$

If $x \in \mathscr{S}_u \subset \mathbb{R}^{n_x}$, then

$$\mathcal{SC} = \psi(u)^\top S_h^{-1} \left[u - \psi(u) + M_h Q_h^{-1} x \right] \ge 0, \tag{17}$$

where $S_h \succ 0$ is any diagonal MF-dependent matrix.

B. LMI-Based Non-PDC Output Feedback Control Design

The following theorem provides sufficient conditions to design a SOF controller (13) that can solve Problem 1.

Theorem 1. Consider the TS fuzzy system (11). If there exist positive definite matrices $Q_i \in \mathbb{R}^{n_x \times n_x}$, diagonal positive definite matrices $S_i \in \mathbb{R}^{n_u \times n_u}$, matrices $M_i \in \mathbb{R}^{n_u \times n_x}$, $F_i \in \mathbb{R}^{n_u \times n_y}$, $G_i \in \mathbb{R}^{n_y \times n_y}$, $K_i \in \mathbb{R}^{n_u \times n_w}$, for $i \in \mathcal{I}_N$, and positive scalars ϵ, γ, α, τ, ρ such that the following optimization problem (18) is feasible:

$$\begin{aligned} \min_{\phi_i, \ i \in \mathcal{I}_N} \quad & \gamma \\ \text{subject to (19), (20), (21) and (22)} & \end{aligned} \tag{18}$$

where $\phi_i = (\epsilon, \gamma, \alpha, \tau, \rho, Q_i, S_i, M_i, F_i, G_i, K_i)$ and

$$\alpha - \tau\phi > 0 \tag{19}$$

$$\begin{bmatrix} Q_i & \star \\ M_{i(l)} & \bar{u}_l^2 \end{bmatrix} \succeq 0, \ \forall l \in \mathcal{I}_{n_u}, \ \forall i \in \mathcal{I}_N \tag{20}$$

$$\begin{bmatrix} Q_j & \star \\ D_i Q_j & \gamma I \end{bmatrix} \succeq 0, \ \forall i \in \mathcal{I}_N, \ \forall j \in \mathcal{I}_N \tag{21}$$

$$\Psi_{iik} \prec 0, \ \Psi_{ijk} + \Psi_{jik} \prec 0, \ \forall i, j, k \in \mathcal{I}_N, \ i < j \tag{22}$$

Then, the non-PDC controller (13) guarantees the closed-loop properties in Problem 1. Moreover, the $\mathcal{L}_\infty-$norm of the output z is minimized. The term Ψ_{ijk} in (22) is given by

$$\Psi_{ijk} = \begin{bmatrix} \Upsilon_{ijk} & \star & \star \\ \rho\mathcal{H}_i^\top & -\rho I & \star \\ \mathcal{L}_{ij} & 0 & -\rho I \end{bmatrix},$$

with

$$\mathcal{H}_i = \begin{bmatrix} 0 & 0 & 0 & H_i^\top & 0 \\ 0 & 0 & 0 & H_i^\top & 0 \\ 0 & 0 & 0 & \epsilon H_i^\top & 0 \end{bmatrix}^\top,$$

$$\mathcal{L}_{ij} = \begin{bmatrix} L_i Q_j & 0 & 0 & 0 & 0 \\ N_i F_j C & -N_i S_j & N_i K_j & 0 & 0 \\ 0 & 0 & 0 & 0 & N_i F_j \end{bmatrix},$$

$$\Upsilon_{ijk} = \begin{bmatrix} \Upsilon_j^{11} & \star & \star & \star & \star \\ \Upsilon_j^{21} & -2S_j & \star & \star & \star \\ 0 & 0 & -\tau I & \star & \star \\ \Upsilon_{ij}^{41} & -B_i S_j & \Upsilon_{ij}^{43} & -Q_k & \star \\ \Upsilon_j^{51} & \epsilon F_j^\top & 0 & \epsilon F_j^\top B_i^\top & \Upsilon_j^{55} \end{bmatrix},$$

and

$$\begin{aligned} \Upsilon_j^{11} &= (\alpha - 1)Q_j, & \Upsilon_j^{21} &= F_j C + M_j, \\ \Upsilon_{ij}^{41} &= A_i Q_j + B_i F_j C, & \Upsilon_{ij}^{43} &= E_i + B_i K_j, \\ \Upsilon_j^{51} &= C Q_j - G_j C, & \Upsilon_j^{55} &= -\epsilon(G_j + G_j^\top). \end{aligned}$$

Proof. Only a sketch of proof is given here due to the lack of space. Based on the convexity property of the membership functions, it follows from (22) that

$$\begin{bmatrix} \Upsilon_{hhh} & \star & \star \\ \rho\mathcal{H}_h^\top & -\rho I & \star \\ \mathcal{L}_{hh} & 0 & -\rho I \end{bmatrix} \prec 0, \tag{23}$$

Note that inequality (23) implies $G_h + G_h^\top \succ 0$. This guarantees that G_h is *nonsingular*, thus the validity of the control expression (13). Applying Schur complement lemma [29], we can prove that (23) is equivalent to

$$\Upsilon_{hhh} + \rho \mathcal{H}_h \mathcal{H}_h^\top + \rho^{-1} \mathcal{L}_{hh}^\top \mathcal{L}_{hh} \prec 0. \tag{24}$$

Let us denote $\mathbf{\Delta}(\kappa) = \text{diag}(\Delta(\kappa), \Delta(\kappa), \Delta(\kappa))$. Since $\mathbf{\Delta}(\kappa)^\top \mathbf{\Delta}(\kappa) \preceq I$, using the following matrix fact:

$$\mathscr{X}^\top \mathscr{Y} + \mathscr{Y}^\top \mathscr{X} \preceq \rho \mathscr{X}^\top \mathscr{X} + \rho^{-1} \mathscr{Y}^\top \mathscr{Y},$$

with $\mathscr{X} = \mathcal{H}_h^\top$ and $\mathscr{Y} = \mathbf{\Delta}(\kappa) \cdot \mathcal{L}_{hh}$, it follows from (24) that

$$\Upsilon_{hhh} + \mathcal{H}_h \mathbf{\Delta}(\kappa) \mathcal{L}_{hh} + \mathcal{L}_{hh}^\top \mathbf{\Delta}(\kappa)^\top \mathcal{H}_h^\top \prec 0. \tag{25}$$

Inequality (25) can be rewritten as

$$\begin{bmatrix} (\alpha-1)Q_h & \star & \star & \star & \star \\ \Upsilon_h^{21} & -2S_h & \star & \star & \star \\ 0 & 0 & -\tau I & \star & \star \\ \hat{\Upsilon}_{41} & \hat{\Upsilon}_{42} & \hat{\Upsilon}_{43} & -Q(h_+) & \star \\ \Upsilon_h^{51} & \epsilon F_h^\top & 0 & \hat{\Upsilon}_{54} & \Upsilon_h^{55} \end{bmatrix} \prec 0, \tag{26}$$

where $\hat{\Upsilon}_{41} = \hat{A}_h Q_h + \hat{B}_h F_h C$, $\hat{\Upsilon}_{42} = -\hat{B}_h S_h$, $\hat{\Upsilon}_{43} = E_h + \hat{B}_h K_h$, $\hat{\Upsilon}_{54} = \epsilon F_h^\top \hat{B}_h^\top$ and $Q(h_+) = \sum_{k=1}^r h_k(\theta(\kappa+1)) Q_k$. Multiplying inequality (26) by

$$\begin{bmatrix} I & 0 & 0 & 0 & 0 \\ 0 & I & 0 & 0 & F_h G_h^{-1} \\ 0 & 0 & I & 0 & 0 \\ 0 & 0 & 0 & I & \hat{B}_h F_h G_h^{-1} \end{bmatrix},$$

on the left and its transpose on the right leads to

$$\begin{bmatrix} (\alpha-1)Q_h & \star & \star & \star \\ \mathcal{X} & -2S_h & \star & \star \\ 0 & 0 & -\tau I & \star \\ \mathcal{Y} & \hat{\Upsilon}_{42} & \hat{\Upsilon}_{43} & -Q(h_+) \end{bmatrix} \prec 0, \tag{27}$$

with

$$\mathcal{X} = F_h G_h^{-1} C Q_h + M_h,$$
$$\mathcal{Y} = \hat{A}_h Q_h + \hat{B}_h F_h G_h^{-1} C Q_h.$$

Applying a congruence transformation to (27), followed by the use of Schur complement lemma, we can prove that (27) is equivalent to

$$\Xi^\top Q(h_+)^{-1} \Xi - \begin{bmatrix} (1-\alpha) Q_h^{-1} & \star & \star \\ \mathcal{Z} & 2S_h^{-1} & \star \\ 0 & 0 & \tau I \end{bmatrix} \prec 0, \tag{28}$$

with

$$\Xi = \begin{bmatrix} A_{cl}(h) & -\hat{B}(h) & E_{cl}(h) \end{bmatrix},$$
$$\mathcal{Z} = S_h^{-1} \left(F_h G_h^{-1} C + M_h Q_h^{-1} \right).$$

Pre- and postmultiplying (28) by $\begin{bmatrix} x^\top & \psi(u)^\top & w^\top \end{bmatrix}$ and its transpose, we obtain

$$\Delta V + 2\mathcal{S}\mathcal{C} + \alpha V(x) - \tau w^\top w < 0. \tag{29}$$

By Lemma 1 with property (17), it follows from (29) that

$$\Delta V + \alpha V(x) - \tau w^\top w < 0, \quad \forall x \in \mathscr{L}_V \backslash \{0\}. \tag{30}$$

Note that inequality (16) follows from (19) and (30). Moreover, by a congruence transformation, followed by the use of Schur complement lemma [29], it follows from (21) that

$$z^\top z = x^\top D_h^\top D_h x \leq \gamma x^\top Q_h^{-1} x \leq \gamma, \ \forall x \in \mathscr{L}_V.$$

Hence, the $\mathcal{L}_\infty-$norm of the output z is bounded by γ. Following a similar procedure, we can prove that condition (20) guarantees $\mathscr{L}_V \subseteq \mathscr{S}_u$. The proof can be now concluded. □

Remark 1. The design conditions in Theorem 1 are reformulated as an optimization problem under LMI constraints with a line search over the scalar ϵ. The control gains F_i, G_i and K_i, for $\forall i \in \mathcal{I}_N$, can be effectively computed using Matlab software with Yalmip toolbox and SDPT3 solver [38].

IV. Illustrative Results and Discussions

This section demonstrates the effectiveness of the proposed fuzzy SOF controller with the high-fidelity CarSim vehicle simulator. The parameters of the CarSim vehicle model considered are $M = 1653$ [kg], $C_f = 95000$ [N/rad], $C_r = 85500$ [N/rad], $l_f = 1.4$ [m], $l_r = 1.646$ [m], and $I_z = 2765$ [kgm^2]. The steer ratio between the driver wheel and the front road steer angle is $R_s = 17.5$. The look-ahead distance to compute the tracking errors is $l_s = 5$ [m]. We assume that the parametric uncertainties in the front and rear tire stiffness coefficients are of 15 %, which represents a highly nonlinear behavior of the lateral tire forces.

Note that the vehicle dynamics (8)–(9) depend on the speed terms v_x, $\frac{1}{v_x}$ and $\frac{1}{v_x^2}$ with

$$v_{\min} \leq v_x \leq v_{\max}, \quad v_{\min} = 5 \text{ [m/s]}, \ v_{\max} = 30 \text{ [m/s]}.$$

If v_x, $\frac{1}{v_x}$ and $\frac{1}{v_x^2}$ are separately considered as premise variables, then the sector nonlinearity approach [15] leads to a T-S fuzzy model with $2^3 = 8$ fuzzy rules. To reduce the numerical complexity, a new premise variable θ is introduced to represent v_x, $\frac{1}{v_x}$ and $\frac{1}{v_x^2}$ as follows [3]:

$$\frac{1}{v_x} = \frac{1}{v_0} + \frac{\theta}{v_1}, \quad v_x \simeq v_0 - \frac{v_0^2 \theta}{v_1}, \quad \frac{1}{v_x^2} \simeq \frac{1}{v_0^2} + \frac{2\theta}{v_0 v_1}, \tag{31}$$

where

$$v_0 = \frac{2 v_{\min} v_{\max}}{v_{\min} + v_{\max}}, \quad v_1 = \frac{2 v_{\min} v_{\max}}{v_{\min} - v_{\max}}.$$

Substituting (31) into (8)–(9), then applying the sector nonlinearity approach, we can obtain a TS fuzzy model of the form (11) with two fuzzy rules to represent the vehicle uncertain dynamics. The details are not given here for brevity. Solving the optimization problem (18) in Theorem 1 with the corresponding vehicle TS fuzzy model, we obtain a path following controller with $\alpha = 0.01$ and $\epsilon = 0.278$. The detail on the obtained control solution is not shown here for brevity. The control performance is now evaluated with a dynamic driving scenario on a race track under highly variable curvatures, road friction and speed conditions.

For CarSim/Simulink co-simulations, the path tracking on a race course track has been conducted with road curvatures varying in the range $\rho_r \in [-0.02, 0.04]$ and the road friction

of $\mu = 0.75$, *i.e.*, $F_{yf} = 2\mu C_f \alpha_f$ and $F_{yr} = 2\mu C_r \alpha_r$. The vehicle traverses the track at dynamic longitudinal speeds in the range $v_x \in [30, 60]$ [km/h]. For regulating the longitudinal speed, the inbuilt PI controller from CarSim has been used. The speed tracking and the path following for the considered driving scenario are shown in Fig. 2. Observe in Fig. 2(a)

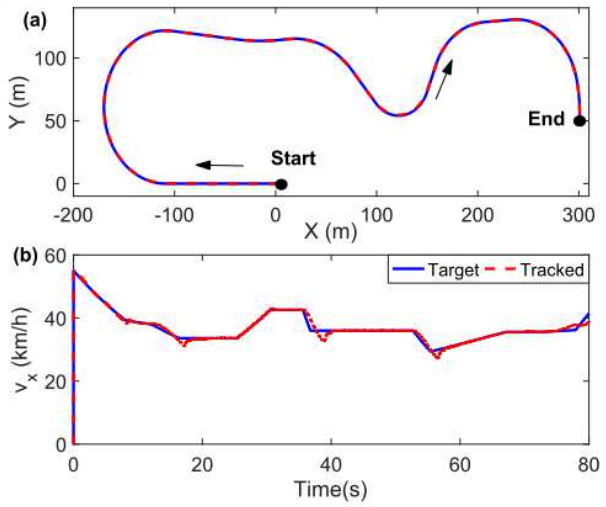

Fig. 2. Tracking performance. (a) Path tracking with the designed TS fuzzy SOF controller, (b) speed tracking using PI controller from the CarSim simulator.

that even without requiring the online measurement of the sideslip angle, the proposed fuzzy non-PDC controller can guarantee an efficient path following under the presence of nonlinear tire forces and uncertainties. Furthermore, the low speed tracking error as depicted in Fig. 2(b) ensures that safe speed limits across a curve are maintained. The lane deviation errors, *i.e.*, lateral error and heading error, are shown in Fig. 3. Remark that the controlled lane errors are small. For comparison analysis, the lane tracking errors with the inbuilt look-ahead preview controller (PC-CSIM) of the CarSim simulator is also illustrated in Fig. 3. Compared to the proposed fuzzy SOF controller (TS-SOF), the lane tracking errors are much larger and cross the lane boundaries, especially at tight curves. Hence, for the considered road friction conditions, the proposed fuzzy SOF controller is able to keep the vehicle on lane which is not the case when using the preview PC-CSIM controller. Subsequently, the illustrations for the vehicle states β, r, the designed steering control input δ and the lateral acceleration are shown in Fig. 4 for both PC-CSIM and fuzzy SOF controllers. It can be seen that the designed control is always within the required constraint of 10 [deg] for both approaches. Further, the sideslip angle does not exceed 0.05 [rad], which ensures that the tire forces are not saturated. With the maximum yaw rate limited by 0.55 [rad/s], the vehicle maintains a stable control performance. In comparison to the PC-CSIM controller, the proposed non-PDC design provide a smooth steering actions, leading to less oscillatory behaviors and a more stable performance in maintaining the state constraints even when the lateral acceleration is high

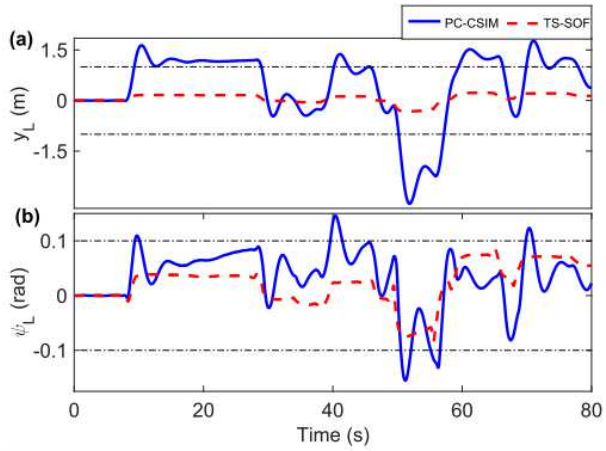

Fig. 3. Path tracking errors. (a) Lateral error y_L, (b) heading error ψ_L.

under the considered friction level.

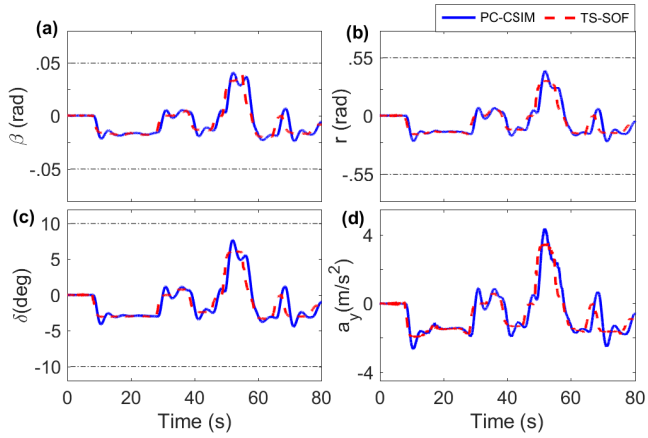

Fig. 4. Vehicle closed-loop behaviors. (a) Sideslip angle β, (b) yaw rate r, (c) designed steering control δ, (d) lateral acceleration a_y.

V. Conclusions

A new LMI-based control solution for autonomous driving has been proposed. The time-varying vehicle speed and the uncertain lateral tire forces are effectively handled using TS fuzzy control. Moreover, the physical limitations on the steering input is explicitly considered in the control design via the robust set-invariance concept and Lyapunov stability theorem. To reduce the design conservatism, fuzzy Lyapunov functions and a non-PDC control scheme are used for theoretical derivations. The practical performance of the new fuzzy SOF path following controller is demonstrated with CarSim/Simulink co-simulations under dynamic driving conditions.

Acknowledgement

This work was done within the ELSAT2020 project, supported by the International Campus on Safety and Intermodality in Transportation, the Hauts-de-France Region, the European Community, the Ministry of Higher Education and Research, and the National Center for Scientific Research.

REFERENCES

[1] A. Broggi, P. Medici, P. Zani, A. Coati, and M. Panciroli, "Autonomous vehicles control in the VisLab intercontinental autonomous challenge," *Annu. Rev. Control*, vol. 36, no. 1, pp. 161–171, Apr. 2012.

[2] S. E. Shladover, C. A. Desoer, J. K. Hedrick, M. Tomizuka, J. Walrand, W. . Zhang, D. H. McMahon, H. Peng, S. Sheikholeslam, and N. McKeown, "Automated vehicle control developments in the PATH program," *IEEE Trans. Veh. Technol.*, vol. 40, no. 1, pp. 114–130, Feb. 1991.

[3] A.-T. Nguyen, C. Sentouh, and J.-C. Popieul, "Fuzzy steering control for autonomous vehicles under actuator saturation: Design and experiments," *J. Franklin Inst.*, vol. 355, no. 18, pp. 9374–9395, Dec. 2018.

[4] B. Paden, M. Čáp, S. Z. Yong, D. Yershov, and E. Frazzoli, "A survey of motion planning and control techniques for self-driving urban vehicles," *IEEE Trans. Intell. Veh.*, vol. 1, no. 1, pp. 33–55, Mar. 2016.

[5] P. Zhao, J. Chen, Y. Song, X. Tao, T. Xu, and T. Mei, "Design of a control system for an autonomous vehicle based on adaptive-PID," *Int. J. Adv. Robot. Syst.*, vol. 9, no. 2, p. 44, Jan. 2012.

[6] J. Naranjo, C. Gonzalez, R. Garcia, T. de Pedro, and R. Haber, "Power-steering control architecture for automatic driving," *IEEE Trans. Intell. Transp. Syst.*, vol. 6, no. 4, pp. 406–415, Dec. 2005.

[7] H. Taghavifar and S. Rakheja, "Path-tracking of autonomous vehicles using a novel adaptive robust exponential-like-sliding-mode fuzzy type-2 neural network controller," *Mech. Syst. Signal Process.*, vol. 130, pp. 41–55, Sept. 2019.

[8] N. Amer, H. Zamzuri, K. Hudha, and Z. Kadir, "Modelling and control strategies in path tracking control for autonomous ground vehicles: a review of state of the art and challenges," *J. Intell. Robot. Syst.*, vol. 86, no. 2, pp. 225–254, May 2017.

[9] J. M. Snider, "Automatic steering methods for autonomous automobile path tracking," Robotics Institute, Carnegie Mellon University, Tech. Rep. CMU-RI-TR-09-08, Feb. 2009.

[10] G. Tagne, R. Talj, and A. Charara, "Design and comparison of robust nonlinear controllers for the lateral dynamics of intelligent vehicles," *IEEE Trans. Intell. Transp. Syst.*, vol. 17, no. 3, pp. 796–809, 2016.

[11] Z. Chu, Y. Sun, C. Wu, and N. Sepehri, "Active disturbance rejection control applied to automated steering for lane keeping in autonomous vehicles," *Control Eng. Pract.*, vol. 74, pp. 13–21, May 2018.

[12] J. Funke, M. Brown, S. M. Erlien, and J. C. Gerdes, "Collision avoidance and stabilization for autonomous vehicles in emergency scenarios," *IEEE Trans. Control Syst. Technol.*, vol. 25, no. 4, pp. 1204–1216, 2017.

[13] H. Guo, C. Shen, H. Zhang, H. Chen, and R. Jia, "Simultaneous trajectory planning and tracking using an MPC method for cyber-physical systems: A case study of obstacle avoidance for an intelligent vehicle," *IEEE Trans. Indus. Inform.*, vol. 14, no. 9, pp. 4273–4283, Sep. 2018.

[14] L. Yang, M. Yue, and T. Ma, "Path following predictive control for autonomous vehicles subject to uncertain tire-ground adhesion and varied road curvature," *Int. J. Control, Autom. Syst.*, vol. 17, no. 1, pp. 193–202, 2019.

[15] K. Tanaka and H. O. Wang, *Fuzzy Control Systems Design and Analysis: A Linear Matrix Inequality Approach*. John Wiley & Sons, 2004.

[16] A.-T. Nguyen, C. Sentouh, and J.-C. Popieul, "Driver-automation cooperative approach for shared steering control under multiple system constraints: Design and experiments," *IEEE Trans. Ind. Electron.*, vol. 64, no. 5, pp. 3819–3830, May 2017.

[17] H. Dahmani, O. Pagès, and A. El Hajjaji, "Observer-based state feedback control for vehicle chassis stability in critical situations," *IEEE Trans. Control Syst. Technol.*, vol. 24, no. 2, pp. 636–643, Mar. 2016.

[18] B. Boada, M. Boada, and V. Diaz, "Fuzzy-logic applied to yaw moment control for vehicle stability," *Vehicle Syst. Dyn.*, vol. 43, no. 10, pp. 753–770, Feb. 2005.

[19] Z. Lendek, T.-M. Guerra, R. Babuska, and B. De Schutter, *Stability Analysis and Nonlinear Observer Design Using Takagi-Sugeno Fuzzy Models*. Springer, Berlin, Heidelberg, Oct. 2011, vol. 262.

[20] A.-T. Nguyen, T. Taniguchi, L. Eciolaza, V. Campos, R. Palhares, and M. Sugeno, "Fuzzy control systems: Past, present and future," *IEEE Comput. Intell. Mag.*, vol. 14, no. 1, pp. 56–68, Feb. 2019.

[21] B. Mansouri, N. Manamanni, K. Guelton, A. Kruszewski, and T.-M. Guerra, "Output feedback LMI tracking control conditions with $\mathscr{H}_\infty$ criterion for uncertain and disturbed T–S models," *Inf. Sci.*, vol. 179, no. 4, pp. 446–457, 2009.

[22] H. Du, N. Zhang, and G. Dong, "Stabilizing vehicle lateral dynamics with considerations of parameter uncertainties and control saturation through robust yaw control," *IEEE Trans. Veh. Technol.*, vol. 59, no. 5, pp. 2593–2597, June 2010.

[23] S. Bezzaoucha, B. Marx, D. Maquin, and J. Ragot, "Contribution to the constrained output feedback control," in *American Control Conference*. IEEE, 2013, pp. 235–240.

[24] A.-T. Nguyen, K. Tanaka, A. Dequidt, and M. Dambrine, "Static output feedback design for a class of constrained Takagi-Sugeno fuzzy systems," *J. Franklin. Inst.*, vol. 354, no. 7, pp. 2856–2870, 2017.

[25] A. Lopes, V. J. Leite, L. Silva, and K. Guelton, "Anti-windup TS fuzzy PI-like control for discrete-time nonlinear systems with saturated actuators," *Int. J. Fuzzy Syst.*, pp. 1–16, 2020.

[26] A.-T. Nguyen, P. Chevrel, and F. Claveau, "Gain-scheduled static output feedback control for saturated LPV systems with bounded parameter variations," *Automatica*, vol. 89, pp. 420–424, Mar. 2018.

[27] A.-T. Nguyen, C. Sentouh, and J.-C. Popieul, "Sensor reduction for driver-automation shared steering control via an adaptive authority allocation strategy," *IEEE/ASME Trans. Mechatron.*, vol. 23, no. 1, pp. 5–16, Feb. 2018.

[28] C. Ting, "An output-feedback fuzzy approach to guaranteed cost control of vehicle lateral motion," *Mechatronics*, vol. 19, pp. 304–312, 2009.

[29] S. Boyd, L. El Ghaoui, E. Feron, and V. Balakrishnan, *Linear Matrix Inequalities in System and Control Theory*. Philadelphia: SIAM, 1994.

[30] A.-T. Nguyen, J. Rath, T.-M. Guerra, R. Palhares, and H. Zhang, "A robust set-invariance approach for constrained path tracking control of autonomous vehicles under dynamic driving maneuvers," *IEEE Trans. Intell. Transp. Syst.*, 2020, In Press.

[31] J. Kim, "Identification of lateral tyre force dynamics using an extended Kalman filter from experimental road test data," *Control Eng. Pract.*, vol. 17, no. 3, pp. 357–367, Mar. 2009.

[32] H. Zhang, X. Zhang, and J. Wang, "Robust gain-scheduling energy-to-peak control of vehicle lateral dynamics stabilisation," *Vehicle Syst. Dyn.*, vol. 52, no. 3, pp. 309–340, Feb. 2014.

[33] R. Rajamani, *Vehicle Dynamics and Control*. Boston: Springer, 2012.

[34] C. Sentouh, A.-T. Nguyen, M. Benloucif, and J.-C. Popieul, "Driver-automation cooperation oriented approach for shared control of lane keeping assist systems," *IEEE Trans. Control Syst. Technol.*, vol. 27, no. 5, pp. 1962–1978, 2019.

[35] S. Tarbouriech, G. Garcia, J. Gomes da Silva Jr., and I. Queinnec, *Stability and Stabilization of Linear Systems with Saturating Actuators*. London: Springer-Verlag, 2011.

[36] A.-T. Nguyen, T. Laurain, R. Palhares, and J. Lauber, "LMI-based control synthesis of constrained T-S systems subject to $\mathcal{L}_2$ or $\mathcal{L}_\infty$ disturbances," *Neurocomputing*, vol. 207, pp. 793–804, Sept. 2016.

[37] G. Da Silva and S. Tarbouriech, "Antiwindup design with guaranteed regions of stability: an LMI-based approach," *IEEE Trans. Autom. Control*, vol. 50, no. 1, pp. 106–111, 2005.

[38] J. Löfberg, "YALMIP: A toolbox for modeling and optimization in Matlab," in *IEEE Int. Symp. Comput. Aided Control Syst. Des.*, Tapei, 2004, pp. 284–289.